

Microscopic Structure of Aqueous Alkylamine mixtures: a Computer Simulation Study

Martina Požar¹, Lena Friedrich², Bernarda Lovrinčević¹,
Michael Paulus², Christian Sternemann² and Aurélien Perera³ *

October 3, 2025

¹Faculty of Science, University of Split, Ruđera Boškovića 33, 21000 Split, Croatia

²Fakultät Physik/DELTA, Technische Universität Dortmund, D-44221 Dortmund, Germany

³Laboratoire de Physique Théorique de la Matière Condensée (UMR CNRS 7600), Sorbonne Université, 4 Place Jussieu, F75252, Paris cedex 05, France.

Abstract

Aqueous alkylamine mixtures are studied by computer simulations in order to understand the microscopic origin of the water rich side prominent x-ray scattering pre-peaks reported in a recent study. These pre-peaks are puzzling in view of the apparently contradicting facts that neat amines show pre-peaks much weaker than neat alkanols, while water-rich aqueous alcohols do not. These observations can be intuitively rationalized by noting that the amine head group have two hydrogen atoms when the hydroxyl group have only one, but they oppose the following two facts: i) computer simulations show micro-heterogeneity for both systems; ii) amines mix with water better than alcohols, both over larger concentrations and alkyl tails lengths.

The study of the atom-atom pair correlation functions and related structure factors allows to understand the microscopic molecular details. The most interesting observation is that the amine head groups accumulate preferentially at the surface of the water domains, and increasingly better with longer alkyl tail, thus allowing to stabilize both the water and alkylamine domains, hence avoiding macroscopic demixing, except at high water concentrations when amines are scarce to achieve efficient surface saturation. The amine domains appear as disordered bilayers. Hence, aqueous amines are analogous to an inverse micelle melt and as precursor micro-emulsion.

*aup@lptmc.jussieu.fr

This stable micro-segregation produces large domain oscillations in the long range part of the correlation functions, translating into positive pre-peaks and negative anti-peaks in the related structure factors, the latter which contribute destructively to produce the prominent scattering pre-peak observed in the x-ray experiments.

The model dependence is shown to be quite important, both for water and solute models. The CHARMM-AA model associated with the SPC/E model seems to be a good compromise.

1 Introduction

Alkylamines are known to be miscible in water¹ both over a large range of concentrations and alkyl chain length. This is in contrast with alkanols, which demix with water beyond 1-propanol and over a much larger concentration range. Interestingly, alkylamines beyond pentylamine show a lower critical solution temperature (LCST). From the interpretation of Walker and Vause,² this indicates strong water-amine dimer type pairing. Another important experimental fact is the large X-ray scattering pre-peaks (SPP) recently reported for several aqueous amine mixtures.³ SPP are often interpreted as a signature of the existence of supramolecular associations. Indeed, SPP are found in several systems such as neat alcohols⁴⁻¹⁴ and amines,¹⁵ room temperature ionic liquids, both neat¹⁶⁻¹⁸ and in aqueous mixing.^{19,20} SPP are equally found in some water-poor aqueous alcohol mixtures, such as aqueous octanol mixtures²¹. However, because of the water strong tendency to self-Hbond, one expects small water clusters in water-poor mixtures, hence such SPP are naturally expected. Conversely, SPP from the water rich side are not obvious to explain because of the complex interplay between the different Hbonding species in presence.

Interestingly, SPP are preferentially found in soft matter systems²² and particularly micro-emulsions.^{23,24} In what concerns us, the SPP in aqueous amines appear to be inconsistent with the following facts: i) neat alcohols have a much better defined SPP than neat amines; ii) water-rich aqueous mixtures of simple alkanols do not show SPP, rather they tend to show large $k = 0$ concentration fluctuation peaks,²⁵⁻²⁷ usually a precursor signature of demixing.²⁸ The difference between $k = 0$ peaks and SPP is an important point related to the difference between concentration fluctuations and micro-heterogeneity, which we have addressed in previous works,²⁹⁻³³ and which we will examine again in the later sections. These questions are best answered through molecular models and computer simulations.

The physics behind SPP is quite simple from the point of view of Coulomb association and charge order in molecular models: the molecular sites of opposite charges tend to associate one another, hence segregating the uncharged (or weakly charged) ones. This is for instance the case in neat alcohol, where the OH hydroxyl head groups self-associate in chain patterns.^{13,14,34-38} In the neat amines, we have shown that the Coulomb association is hindered by the dual hydrogen atoms of the amine head group, leading to weaker SPP.¹⁵ In aqueous mixing conditions, water enters the competition of Coulomb associations. It is

intuitively easy to imagine that the dual hydrogens of the amine groups are now an advantage to associate with water, supporting the dimer picture of Walker and Vause. However, it does not explain the prominent SPP in a simple intuitive way.

The purpose of the present work is to examine the micro-structure of aqueous amines for several amines ranging from propylamine to octylamine, and for different water and amine models. All models show that aqueous amine mixtures have considerable micro-heterogeneity, somewhat similar to other aqueous mixtures, but which do not necessarily show SPP, hence indicating that SPP and micro-segregation are not necessarily equivalent. This can be explained only through the analysis of atom-atom pair correlations, both in direct and reciprocal space.

To our knowledge, there are very few simulation studies focusing purely on the structuring in aqueous amines. Kusalik and co-authors published a paper on the local structure in neat methylamine and methylamine-water mixtures.³⁹ The work of Lachet and colleagues centered on the development of force fields of primary, secondary, and tertiary amines,^{40,41} which were then put to use in studies about equilibrium and transport properties of neat amines⁴² and gas solubility in amines.⁴³

The remainder of this paper is as follows. In the next section we study theoretical and methodological aspects (simulations). In the third section we discuss the special type of micro-segregation observed in simulations of aqueous amines. In the fourth section we study how correlation functions help understand the micro-structure of these mixtures. A discussion and conclusion sections close this paper.

2 Theoretical and technical considerations

2.1 Scattering intensity and density pair correlation functions

The experimental x-ray scattering intensity for a binary mixture can be readily obtained from the total atom-atom structure factors $S_{i_a j_b}^{(T)}(k)$, where a, b are molecular species indices and i_a, j_b are atom index, through the Debye formula:^{44,45}

$$I(k) = r_0^2 \rho \sum_{ab} \sqrt{x_a x_b} \sum_{ij} f_{i_a}(k) f_{j_b}(k) S_{i_a j_b}^{(T)}(k) \quad (1)$$

where the $S_{ij}^{(T)}(k)$ are defined as:

$$S_{i_a j_b}^{(T)}(k) = w_{i_a j_b}(k) \delta_{ab} + \rho H_{i_a j_b}(k) \quad (2)$$

where the $w_{i_a j_b}(k)$ are the intra-molecular structure factors (which imposes $a = b$, since these exists only within the same molecule, hence the Kronecker symbol δ_{ab}), $\rho = N/V$ is the total number density (where $N = N_a + N_b = N_1 + N_2$

is the total number of molecules and V the volume), $x_a = N_a/N$ is the mole fraction of species a (with notation $a = 1, 2$ for a binary mixture), and the $H_{i_a j_b}(k)$ related to the Fourier transform of the atom-atom intermolecular pair correlation function $g_{i_a j_b}(r)$

$$H_{i_a j_b}(k) = \sqrt{x_a x_b} \int d\vec{r} [g_{i_a j_b}(r) - 1] \exp(i\vec{k} \cdot \vec{r}) \quad (3)$$

In addition to $S_{i_a j_b}^{(T)}(k)$, we introduce the atom-atom structure factor void of the intra-molecular contributions (the self structure factors - see next sub-section)

$$S_{i_a j_b}(k) = \delta_{i_a j_b} + H_{i_a j_b}(k) \quad (4)$$

which are the quantities which will be discussed in this paper.

The functions $g_{i_a j_b}(r)$ are calculated directly from the GROMACS trajectory files (using the gmx rdf program), while the intra-molecular parts $w_{i_a j_a}(r)$ are calculated as described in Ref.¹³ by sampling the mean atom-atom distance histograms within each molecules in several configurations.

2.2 Duality of concentration fluctuation and micro-heterogeneity

The functions $g_{i_a j_b}(r)$ can be seen as atom pair *distribution* functions, but they are also defined as pair *correlation* functions in a statistical sense.

In the first case, the $g_{i_a j_b}(r)$ can be evaluated through the histogram of the atom-atom spatial distributions in the molecular configurations

$$g_{i_a j_b}(r) = \frac{H_{i_a j_b}(r, \delta r)}{N_i^2 \delta V(r, \delta r)} \quad (5)$$

where $H_{i_a j_b}(r, \delta r)$ is the number of atoms j_b in a spherical shell of radii r and thickness δr , centered on atom i_a , N_i is the number of molecules of species i in a volume V , and $\delta V(r, \delta r) = (4\pi r^2 \delta r)/V$ is the normalized volume of the shell. This is done through the GROMACS program.

In the second case, the $g_{i_a j_b}(r)$ are related⁴⁶ to the second statistical moment of the random variable $\rho_{i_a}(\vec{r})$, which is the microscopic atom density of atom i_a defined as:

$$\rho_{i_a}(\vec{r}) = \sum_{n_a} \delta(\vec{r} - \vec{r}_{n_a}) \quad (6)$$

The first moment is the one-body function $\rho_{i_a}^{(1)}(\vec{r})$, which, in the absence of any external field, is just the number density ρ_{i_a} of atom i_a :

$$\rho_{i_a}^{(1)}(\vec{r}) = \langle \rho_{i_a}(\vec{r}) \rangle = \frac{N_{i_a}}{V} = \rho_{i_a} \quad (7)$$

where N_{i_a} is the number of atoms of type i_a , and $\langle \rangle$ designates a statistical ensemble average.

The second moment is the two-body function function $\rho_{i_a j_b}^{(2)}(\vec{r}_1, \vec{r}_2)$ defined as

$$\rho_{i_a j_b}^{(2)}(\vec{r}_1, \vec{r}_2) = \langle \rho_{i_a}(\vec{r}_1) \rho_{j_b}(\vec{r}_2) \rangle \quad (8)$$

This function is related to the static van Hove function⁴⁶ and can be split into a self part ($i_a = i_b$) and a distinct part ($i_a \neq i_b$) by using Eq.(6) and separating the two types of index contributions. The self part contributes to the intramolecular function⁴⁷ and the distinct part.

The pair correlation function $g_{i_a j_b}(\vec{r}_1, \vec{r}_2)$ can be introduced from the distinct part $\rho_{D; i_a j_b}^{(2)}(\vec{r}_1, \vec{r}_2)$ through the obvious meaning of what a correlation is:

$$\rho_{D; i_a j_b}^{(2)}(\vec{r}_1, \vec{r}_2) = \rho_{i_a}^{(1)}(\vec{r}_1) \rho_{j_b}^{(1)}(\vec{r}_2) g_{i_a j_b}(\vec{r}_1, \vec{r}_2) \quad (9)$$

Indeed, at large separations, this function should obey the relation

$$\lim_{|\vec{r}_2 - \vec{r}_1| \rightarrow \infty} \rho_{D; i_a j_b}^{(2)}(\vec{r}_1, \vec{r}_2) = \rho_{i_a}^{(1)}(\vec{r}_1) \rho_{j_b}^{(1)}(\vec{r}_2) \quad (10)$$

thus implying the well know limit for the correlation term

$$\lim_{|\vec{r}_2 - \vec{r}_1| \rightarrow \infty} g_{i_a j_b}(\vec{r}_1, \vec{r}_2) = 1 \quad (11)$$

In the absence of an external field, the system is uniform and isotropic, thus this function depends only on the module of the relative distance $r = |\vec{r}_2 - \vec{r}_1|$, and the correlation function naturally reduces to $g_{i_a j_b}(r)$ which can be written from Eqs.(7,9) as

$$g_{i_a j_b}(r) = \frac{1}{\rho_{i_a} \rho_{i_b}} \rho_{D; i_a j_b}^{(2)}(r) \quad (12)$$

Equation (8) shows an important feature, that the pair correlation function is related to the fluctuations of the microscopic order parameters $\rho_{i_a}(\vec{r})$. In that sense, they monitor the local and global stability of the system.⁴⁸ This is most efficiently seen through the small- k behaviour of the structure factors $S_{i_a j_b}(k)$ introduced in Eq.(4), the $k = 0$ values of which are related to the isothermal compressibility.^{46, 49, 50} The Kirkwood-Buff theory shows that the concentration fluctuations in the system are related to the integrals of the pair correlation functions.

What is generally observed is the following. When a mixture tends to phase separate, then the concentration fluctuations are large, their correlation range increases and this translates through Eqs.(3,4) into a $k = 0$ growth of a peak in the structure factors. However, when micro-heterogeneity and domain formation occurs, then it is a positive small- k peak that appear for like species, usually accompanied by a negative cross correlation anti-peak for unlike species.^{16, 51, 52} In some systems, such as alcohol/ionic-liquid mixtures,⁵³ both phenomena are observed, which means that stable micro-segregation can transform into macroscopic phase separation when parameters such as concentration or temperature are tuned. The $k = 0$ peak could be considered as a packing of molecules in growing cluster, hence a classical boson analogy. Conversely, the stable separation of antagonist nano-domains could be considered a a classical fermion analogy. We previously suggested this analogy in the context of aqueous-dioxane mixtures.³³

2.3 Computer simulation technical details

The results presented in this work were obtained by molecular dynamics simulations in the GROMACS program package.⁵⁴ We tested several force fields for amines in order to reproduce the experimental results of aqueous amine mixtures. We first tested united-atom models of amines Gromos 53a6,⁵⁵ Gromos 54a7⁵⁶ and OPLS-UA,^{57,58} which failed to yield miscibility with water. After that, we turned to CHARMM all-atom^{59–61} and OPLS-AA,^{57,62} which produced miscibility with the SPC/e water model,⁶³ but also with the TIP4P_2005 model.⁶⁴

All aqueous amine mixtures contained 16000 molecules, the starting configurations of which were generated with Packmol.⁶⁵ After obtaining the initial configurations, we followed the same simulation protocol: energy minimization and equilibration for 10 ns, followed by production runs of 10 ns, during which at least 2000 configurations were collected. All simulations were performed in the NpT ensemble, with the pressure $p = 1$ bar and the temperatures of $T = 300$ K and $T = 340$ K. The temperature was maintained with the v-rescale thermostat⁶⁶ and the pressure with the Parrinello-Rahman barostat.^{67,68} The temperature algorithm had a time constant of 0.2 ps and the pressure algorithm was set at 2 ps. The short-range interactions were calculated within the 1.5 nm cut-off radius, while the long-range electrostatics were calculated with the PME (Partial Mesh Ewald) method.⁶⁹ The LINCS algorithm⁷⁰ handled the constraints.

3 Mixing with nano-domain formation

The experimental phase diagram from Glinsky et al.⁷¹ is sketched in Fig.SI-1 of the SI document, for aqueous hexylamine and octylamine. One can see that both phase diagrams have a UCST (upper critical solution temperature) behaviour, which means the existence of a supra-structural organisation.²

Fig.1 illustrates what is perhaps the most astonishing result of the computer simulations of aqueous alkylamines: that the nitrogen atoms saturate the surface of the micro-segregated water domains, hence contributing to stabilizing them. We believe that this is the first time that this is shown for aqueous amines. All snapshots show one face of the simulation box, chosen randomly, of a 20% amine mixture in water. The upper right panel shows aqueous ethanol (TraPPE model) for comparison. The ethanol oxygen are shown in blue and it can be seen that these are uniformly distributed throughout the segregated ethanol domains. All other panels show alkylamines (CHARMM-AA model), from propylamine in (b) up to octylamine in (f). While for propylamine it is not obvious that the amine head groups are saturating the water domains, this become quite clear starting from butylamine in panel (c).

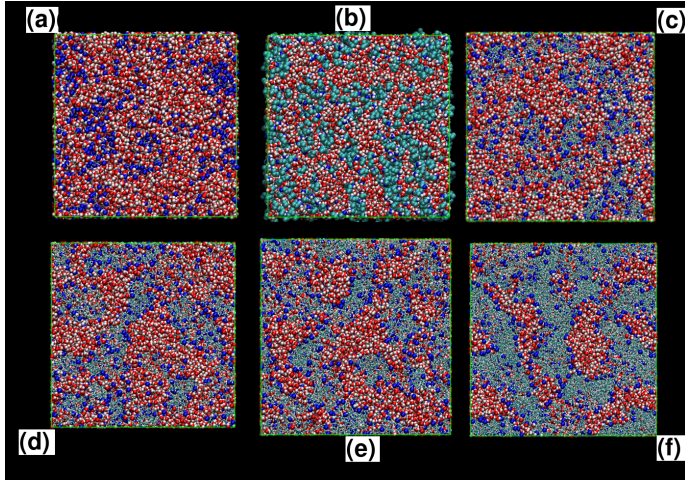


Figure 1: Snapshots of one randomly chosen face of the simulation cubic box for several aqueous mixtures of 20% solutes. Panel (a) is for aqueous ethanol (TraPPE model), panels (b) to (f) are for propylamine to octylamine (skipping heptylamine), respectively. Water is shown with oxygen in red and hydrogen in white. The amine nitrogen is highlighted in blue, while all other amine atoms are shown in semi-transparent cyan. Ethanol oxygen in (a) is shown in blue, and the propylamine alkyl tail in (b) is shown in full atom representation (cyan).

As the alkyl chains grow in length, the water domains shrink, but the nitrogen atoms continue to saturate their surface, with very little amine head inside the alkyl domains. This is consistent with the fact that neat alkylamines do not form specific large amine head group clusters,⁷² while neat alkanols tend to form nice chain clusters.^{34,35}

The spacing between the water domains is more or less about two alkyl tail lengths, which would be consistent with a disordered alkylamine bilayer system. Indeed, at low temperature, experiments show that such bilayers are formed. Fig. 2 shows such a layer system for a 10% hexylamine aqueous mixture at 10 °C, and how such bilayers remain stable despite some fluctuations. The amine bilayers are such that the amine head groups stick on both sides to the upper and lower water layers.

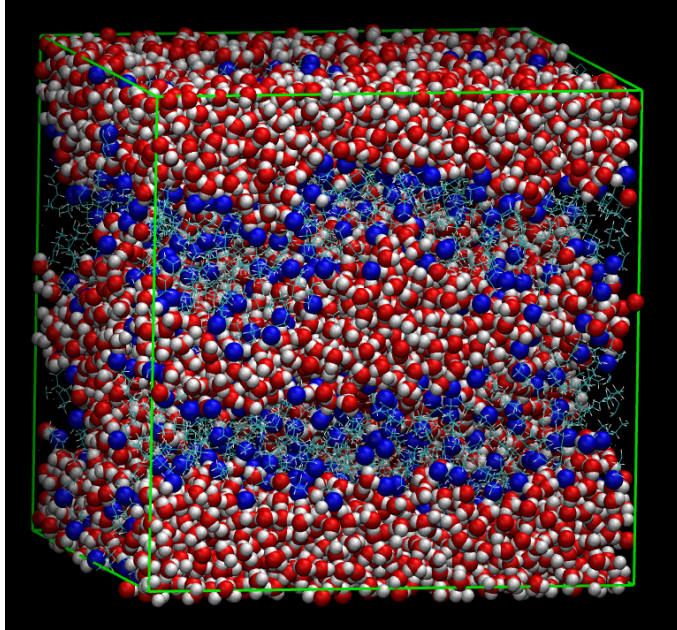


Figure 2: Snapshot of a low temperature ($10\text{ }^{\circ}\text{C}$) hexylamine-water bilayer system. The atom color follow the same conventions as in Fig.1.

As temperature is increased, these bilayers get disorganized and form random micro-emulsions type patterns observed in Fig. 1. At low amine densities, when the water domains tend to be large, there are not enough amine head groups to stabilize them and the system demixes.⁷¹

Interestingly, the low amine content demixing range increases with temperature, which is a scenario consistent with the LCST found in experiments.¹ Indeed, as temperature increases the water domain become more disordered, hence larger, which makes it even more difficult for the amine head groups to cover them.

The amine concentration dependence of the microstructure is illustrated in Fig. 3 for the case of hexylamine. It is clearly seen that the water domains shrink as the amine concentration increases. But the nitrogen atom saturation of the domains is preserved, even if for large amine concentrations many nitrogen atoms appear in the bulk of the amine domains.

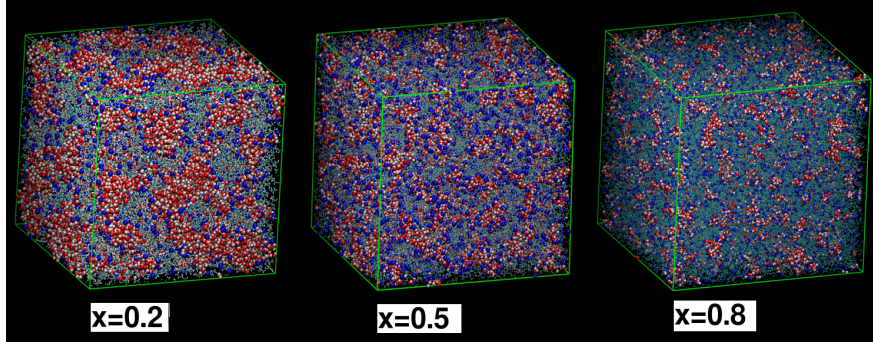


Figure 3: Evolution of the domain structure with amine concentration x , for the aqueous hexylamine systems. Atom coloring conventions as shown in Fig.1 . The alkyl tails are represented in semi-transparent modes, with color codes adapted to enhance domain size and structure differences.

How does this microstructure translate into the various atom-atom pair correlation functions? This is examined in the next section.

4 Microscopic description from density pair correlations

Since there are several atoms involved, it is necessary to sort out which atom pairs are most relevant. Indeed, an all-atom description of hexylamine requires 120 atom pairs. Below we examine selectively the various combinations of correlations between the following atoms, the water oxygen atom O_W , the amine nitrogen atom N and the first C_1 and last (tail) C_T atoms. This way, we can have a good idea of the disordered layer type correlations. Perhaps the most interesting aspect is the long range domain correlations, which correspond to the stable micro-heterogeneity observed in Fig. 1. These are the correlations which are responsible for the SPP. We have hinted to the existence of such features in aqueous 1-propanol mixtures.⁷³ But, the absence of SPP for these mixtures, did allow to further develop the research along these lines. Aqueous amine mixtures appear to be the missing link between solutions and soft matter. It is therefore important to understand how one of the most important observables from computer simulations behave for this type of liquid mixtures. In particular, the relation to the dual fluctuation/micro-heterogeneity discussed in Section 2.2 needs some support from the analysis of the correlation functions.

4.1 Pair correlation functions of the H-bonding groups

Because of the existence of dual type of distributions, namely the usual first few neighbour molecular dispositions as well as long range domain correlations, we will focus on both aspects. We will consider how these uncommon second

types of domain correlations settle as the alkyl tails of the amines are made longer and longer, from propylamine to octylamine. For this purpose, we focus on $T = 300$ K mixtures with amine mole fraction $x = 0.2$. We will study charge-charge correlation of the water and amine head groups, as well as those involving neutral alkyl tail atoms.

Fig. 4 shows the pair distributions from the three principal Hbonding atoms pairs, namely oxygen-oxygen $g_{O_w O_w}(r)$ functions for water, nitrogen-nitrogen $g_{NN}(r)$ for amines, and the cross correlations $g_{O_w N}(r)$. These are represented in an unusual log-log plot (see Fig.SI-2 for a more conventional view), in order to magnify at the same level both the large short range correlations due to immediate Hbond neighbour interactions, and the long ranged domain correlations.

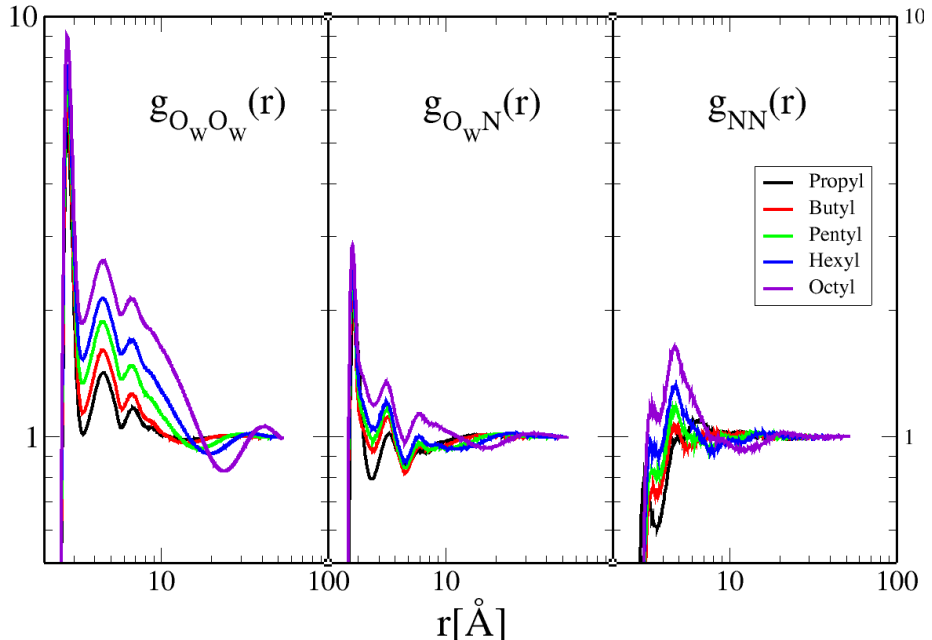


Figure 4: Selected atom-atom correlation functions (in log/log) for various alkylamine-water mixtures for amine mole fraction $x = 0.2$. The domain oscillations (magnified by the log-log plot) are quite visible through the water-water correlation (left panel), specially for longer amines, with domain size about 12nm. For comparison, the semi-log plots are shown in the SI in Fig-SI-1.

The comparison of the left and right panels shows that the water-water correlations are stronger than the solute amine-amine correlations, which is also observed in alcohol-water mixtures.^{74,75} A striking feature is the high first peak of $g_{O_w O_w}(r)$ compared with the much smaller Hbond N-N peak at $r \approx 4\text{\AA}$ in $g_{NN}(r)$, the latter which is even smaller than the broader main peak at $r \approx 4\text{\AA}$, thus indicating that nitrogen atoms nearby to other nitrogen atoms are not

always Hbonded, which is not the case for water. The middle panel for $g_{O_{WN}}(r)$ confirms that there are strongly Hbonded O-N pairs, even if the corresponding correlations are about three times smaller than water-water Hbonds.

The atom-atom structure factors corresponding to the pair correlation functions above are shown in Fig.5. Perhaps the most spectacular feature is the fact that the water-water structure factors for all solutes are nearly indistinguishable from that of neat water in the first peak k -range and beyond $k > 1.5\text{\AA}$. The split feature is the same, with the H-bond peak at $k \approx 2\text{\AA}$ and the contact peak at $k \approx 3\text{\AA}$. This is an outstanding feature because of the following two implications. First, it means that water preserves its bulk type Hbonding even in presence of solutes of different types. Second, one can therefore decouple the small- k and in particular the pre-peak features from both the pair correlation function and its structure factor in the following way

$$g_{WW}(r) = g_W(r) + g_{LR}(r) \quad (13)$$

$$S_{WW}(k) = S_W(k) + S_{PP}(k) \quad (14)$$

where $g_W(r)$ and $S_W(r)$ are the neat water atom-atom pair correlation and structure factor, respectively, for every atom pair OO OH and HH, and $g_{LR}(r)$ is essentially the long range feature (together with remaining small range details), and $S_{PP}(k)$ is the corresponding Fourier transform. These two features, which are important for self-assembly, will be studied in greater details in a companion paper.⁷⁶

In contrast to the water-water correlation functions, the cross correlations (middle panel) and solute-solute correlations show mixed contributions that cannot be detached so clearly as for water, even though this could be formally possible. The enormous difference in magnitude of the pre-peaks between the water and the other contribution is an additional signature of the importance of water preserving its bulk structure. The pre-peaks are direct consequence of the domain oscillatory features observed in Fig.4 in the long range parts of the pair correlation functions.

Fig. 6 shows an important feature of the domain correlations, which is the fact that the water-amine cross domain correlations (red) are in phase opposition with the water-water (black) and amine-amine (green) correlations.

It is this important feature which leads to the cancellations of the prominent partial species contributions to the radiation scattering, leading themselves to a reduced but still prominent scattering pre-peak, as will be discussed later in Section 7 .

It is equally important to study the Hbonding correlation between water and the solutes. This is sketched in Fig. 7.

The H atom correlations reported in Fig. 7 and corresponding to various Hbonding patterns, illustrated in the case of aqueous 20% hexylamine, confirm the deductions above, that water-water correlations (black) are the most prominent, followed by water-amine Hbonding (red). Of the two remaining lesser Hbonding the amine-amine (blue) is nearly featureless, witnessing very little Hbonding. It is remarkable that the water-amine HN Hbonding is so much

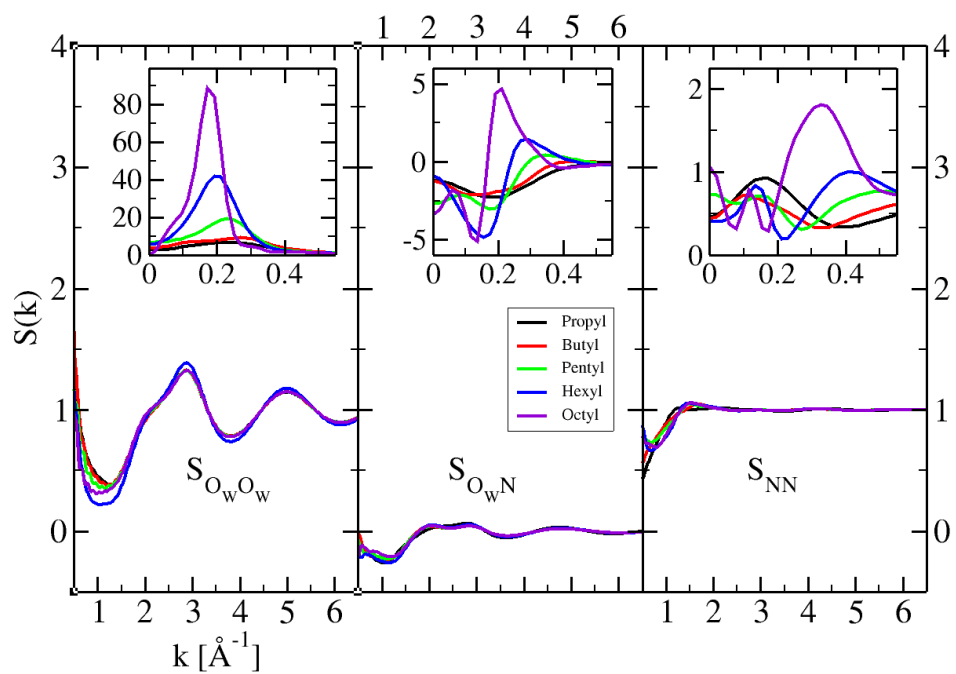


Figure 5: Structure factors corresponding to the pair correlation functions in Fig.4, with same color conventions.

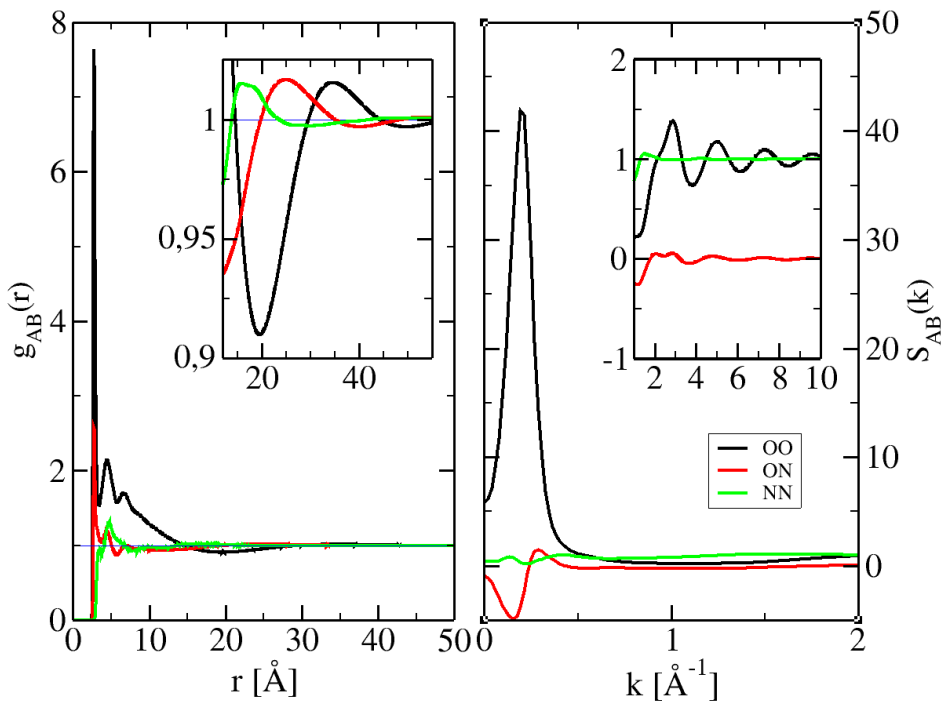


Figure 6: Short range correlations versus domain correlations, illustrated for the case of 20% aqueous hexylamine mixtures, with correlations between the water oxygen O_W and amine nitrogen N (see inset for color conventions). Left panel shows the short range correlations in the main panel and the long range domain oscillations in the inset. Right panel shows small- k SPP features in the main panel and larger k features in the inset.

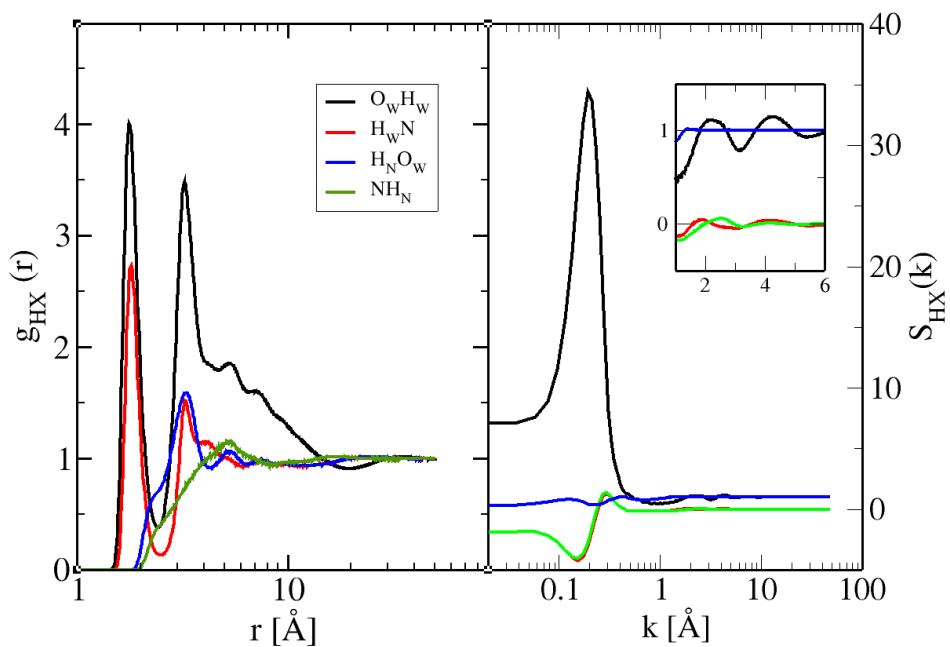


Figure 7: Hydrogen atom correlations between water H_W and amine H_N atoms with water oxygen O_W and amine nitrogen N atoms. Left panel shows the $g(r)$ and right panel the corresponding $S(k)$. The inset shown a zoom around the main peak at $k \approx 2 - 3 \text{\AA}^{-1}$.

more important than the amine-water HNO, indicating that the water-amine dimer through the O-H-N is quite strong. This must be detected in Raman optical spectroscopy measurements, although we are not aware of any such result.

All correlations increase in magnitude with longer alkyl chains, which is a direct consequence of their hydrophobicity helping the mutual confinement of the respective water and amine domains. This is the origin of the micro-heterogeneity, equally observed in aqueous mixtures of smaller alkanols,⁷⁷⁻⁸¹ but which is replaced by full demixing for longer alkanols. Instead, the long range correlations seen in Fig.1 for all three correlation functions, suggest that it is the mechanism behind these correlations that prevents full demixing.

4.2 Pair correlations involving alkyl tails

In this section, we examine how the water oxygen O and amine nitrogen N atoms correlate with the hydrophobic tails, typically the first C_1 and last tail C_T carbon atoms. Then, we also examine how the tail carbon atoms correlate between themselves.

4.2.1 Charged groups correlations with the first carbon atom of the alkyl tails

We first examine the water oxygen O and amine nitrogen N correlation with the hydrophobic first alkylamine carbon atom C_1 . In Fig.8, the upper left panel shows the $g_{OC_1}(r)$ functions for the various alkylamines while the right panel shows the $g_{NC_1}(r)$. What is quite apparent is that only the first neighbour correlations are prominent, as in usual liquids, and the domain correlations are quite small. While this is consistent for the $g_{NC_1}(r)$, in view of the large domain correlations of the $g_{ON}(r)$ in Fig.4, one would have expected similar domain correlations in the $g_{OC_1}(r)$ since the C_1 atom is close to the amine head group. In fact, the near similarities between $g_{OC_1}(r)$ and $g_{NC_1}(r)$ indicates that the water molecules form tight dimers with the N atoms and are only indirectly correlated to the C_1 atoms.

Nevertheless, we do observe depletion correlations of the second neighbours, specially for longer amines (purple curve for octylamine for instance), which is a trace of the interfaces formed by the water and amine head group atoms. The structure factors $S_{OC_1}(k)$ and $S_{NC_1}(k)$ shown in the two lower panels confirms the observations made for the respective $g(r)$ functions. For the amine-amine structure factors we find weak pre-peak due to the Hbonding structures, as in the case of the neat amines.¹⁵ For the water-carbon structure factor we find the typical charge order pre-peak/anti-peak correlations. We note that both structure factors contribute only weakly to the pre-peak, unlike those for the charged groups seen in the insets Fig. 5.

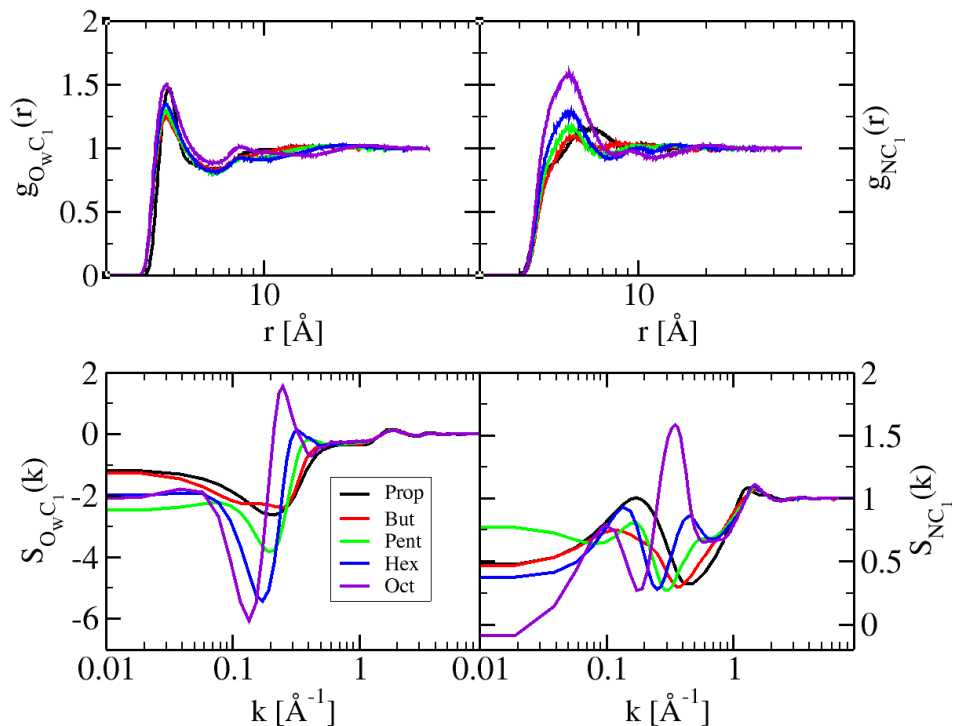


Figure 8: Correlations between the charged atoms (water oxygen O and amine nitrogen N) with the first carbon atom C_1 of the alkyl tails, from propylamine to octylamine. The $g(r)$ functions are shown in the upper panel, and the $S(k)$ functions are shown in the lower panels, left for water and right for amine. The alkylamine color conventions for the curves are shown in the legend box of the lower left panel.

4.2.2 Charged atom correlations with the last carbon atom of the alkyl tails

We expect anti-correlation between the charged groups and the last alkyl tail carbon atom, because of the hydrophobicity between the two segments, and this is what comes out Fig. 9.

What is quite apparent in upper left panel is that the $g_{O_W C_T}(r)$ are dominated by the domain correlations (large oscillations) while the neighbouring atom correlations are the small wiggles (same range as in Fig. 8 for instance), and the latter which are seen to be more prominent for smaller amines and much less as the alkyl tail length increases. Conversely, the domain correlations are seen to increase in the opposite direction. Both features make sense, since we expect more domain correlations for larger alkylamines. The lower left panel shows the corresponding structure factors $S_{O_W C_1}(k)$. We see very clearly that the large tail oscillations contribute to the larger negative anti-peaks, more so as the alkylamine tails size increase. The negative anti-peak indicates that the water oxygen/amine carbon atoms are depleted and in phase opposition with the charge atoms correlations of Fig. 4 and Fig. 5.

We now turn to similar charged/uncharged atom correlations but within the alkylamine molecules. The right panels show the nitrogen/first carbon correlations, $g_{N C_1}(r)$ in the upper one, and $S_{N C_1}(k)$ in the lower one. Here, we observe only neighbouring atom correlations, as in any standard liquids, and the domain correlations are very small. This is consistent with what we observed in a previous work for the neat alkylamines,¹⁵ namely that the negative anti-peak correlations were quite weak when compared with neat alcohols. Indeed, the lower panel shows smaller pre-peak amplitudes than that in the left panel for the oxygen/carbon atoms (as witnessed by the different verticals between the two lower panels).

4.2.3 Carbon-carbon correlations

The correlations between the first C_1 and last C_T carbons are shown in Fig. 10 and for different amines, in log scale for the x-axis. The examination of the $g(r)$ functions in the three upper panels reveals a striking observation, that the $C_T - C_T$ tail atom correlations dominates the other two by a factor 10 (y-axis in log scale). This is a remarkable finding since it proves the layering hypothesis of the alkyl domains. Indeed, if the micro-segregated alkyl domains are constrained by the binding of the O_W and N atoms, then it necessarily means that the bilayer structure must be more or less preserved, even in disordered form. This enforces the correlations between the last carbon atoms, and this is exactly what the $g_{C_T C_T}(r)$ show, and for all amines.

This observation is further supported by the fact that the long range correlations of the $g_{C_T C_T}(r)$ large domain correlations, which is much less the case for the two other functions. Indeed, it is only natural that the last carbon atom witnesses the segregation of the alkyl tail domains from the water domains. The structure factors in the lower row of Fig. 10 confirm these findings. Indeed, the

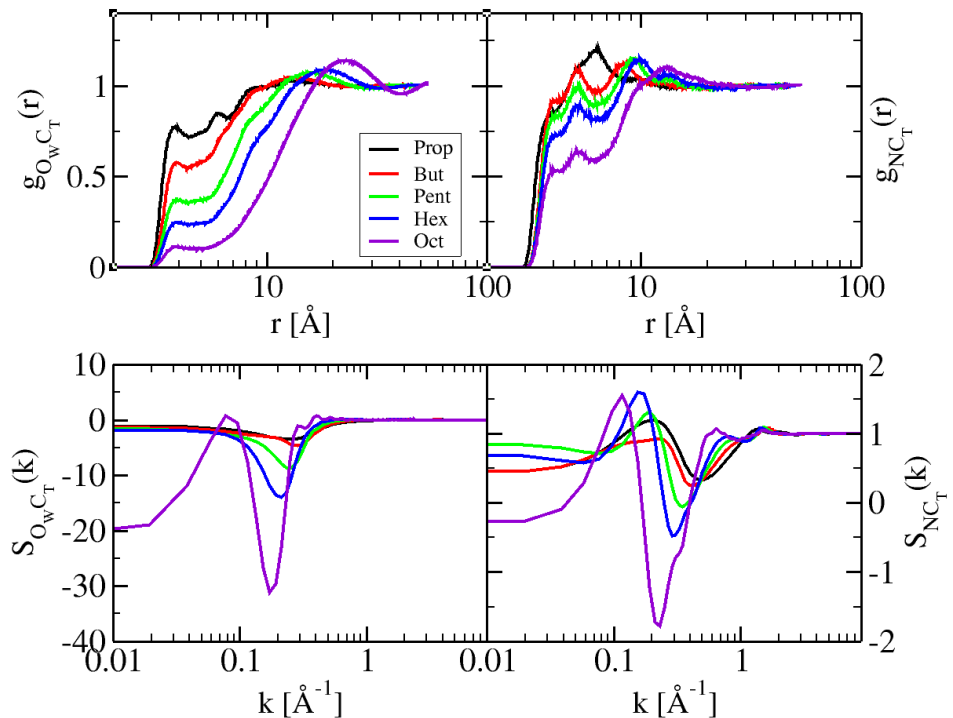


Figure 9: Correlations between the charged atoms (water oxygen O and amine nitrogen N) with the last carbon atom C_T of the alkyl tails, from propylamine to octylamine. The $g(r)$ functions are shown in the upper panel, and the $S(k)$ functions are shown in the lower panels, left for water and right for amine. The alkylamine color conventions for the curves are shown in the legend box of the upper left panel.

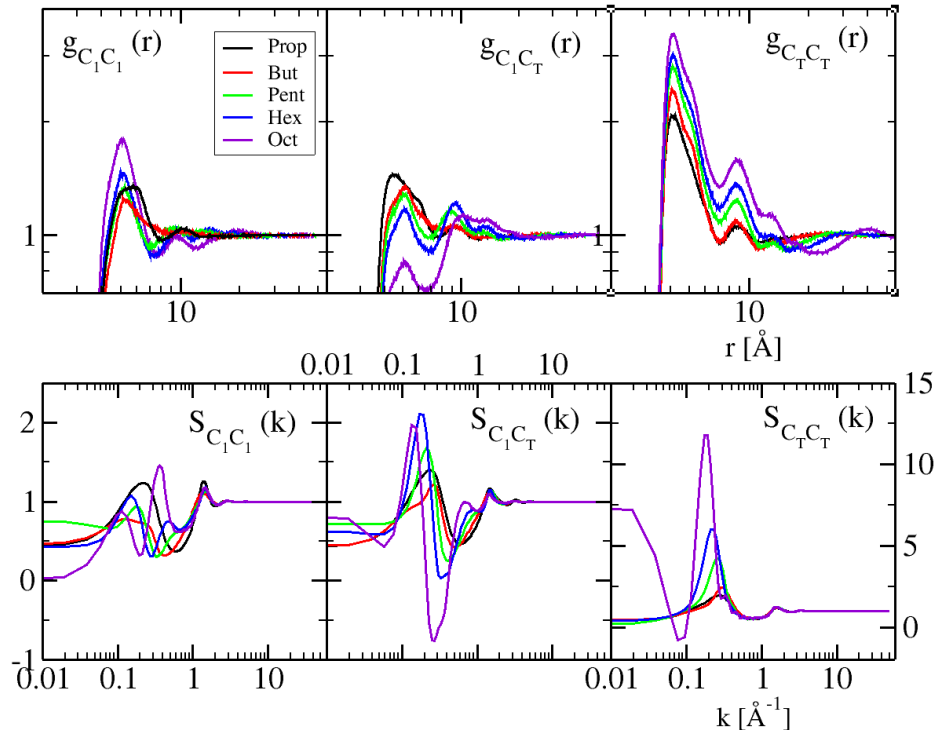


Figure 10: Correlations combinations between the first C_1 and the last C_T carbon atoms of the alkyl tails, from propylamine to octylamine. The $g(r)$ functions are shown in the upper panel, and the $S(k)$ functions are shown in the lower panels, left for water and right for amine and cross correlations in the middle. The alkylamine color conventions for the curves are shown in the legend box of the upper left panel.

amplitude of the pre-peaks for the tail atom $S_{C_T C_T}(k)$ are about 10 times more prominent than the two others, and more so for the longer amines.

Carbon-hydrogen correlations of the alkyl tail atoms are shown in the SI document, in Fig.SI-3 for the $g(r)$ and Fig.SI-4 for the $S(k)$. These plots show clearly that the methyl groups closer to the amine head group witness domain order more readily than the middle or tailing groups. Also the carbon correlations dominate somewhat the hydrogen and carbon-hydrogen correlation, which justifies to some extent the united atom representation.

5 Concentration and temperature dependence

So far we have examined only the 20% amine content between different amines and for room temperature conditions. Since the phase diagrams of the aqueous amines are available from experiments, it is interesting to see how the simulations reproduce concentration and temperature dependence's. We will illustrate this for the case of aqueous hexylamine mixtures for the amine CHARMM-AA model.

5.1 Concentration dependence

Fig.11 shows the room temperature hexylamine (CHARMM-AA) concentration dependence for the correlations between charged atoms pairs O_W and N . Perhaps the most intriguing feature is the fact that the short range correlations ($r < 10\text{\AA}$) have amplitudes increasing with amine concentrations, and for all three $g(r)$ functions, while in the panels below, the pre-peaks and anti-peaks of the structure factors show the opposite behaviour. This is because these pre-peaks reflect the large r domain correlations, which are farther long ranged as the amine concentration *decreases*.

These findings are in line with those observed in the snapshots of Fig. 3: the domain correlations start at larger distances for the smaller amine concentration, since the water domains are larger. Finally, we see that the like atom correlations produce positive pre-peaks, while the cross atom correlations (middle panel) produce negative anti-peaks. As the water concentration becomes smaller, the amine correlation functions tend to look more like those of neat amine.¹⁵

5.2 Temperature dependence

The temperature dependence of the correlations is illustrated for the case of hexylamine in Fig. 12 and for two temperatures, namely room temperature $T = 300$ K and higher temperature $T = 340$ K. Short range correlations ($r < 5\text{\AA}$) have more amplitude at lower temperature than at the higher one, which is a trend generally observed for simple liquids, since lower temperature means denser systems and increased correlations. However, at medium distances ($5\text{\AA} < r < 10\text{\AA}$) we observe a clear increase of correlations. At even greater distances (left inset), we observe a small shift of the domain correlation oscillations

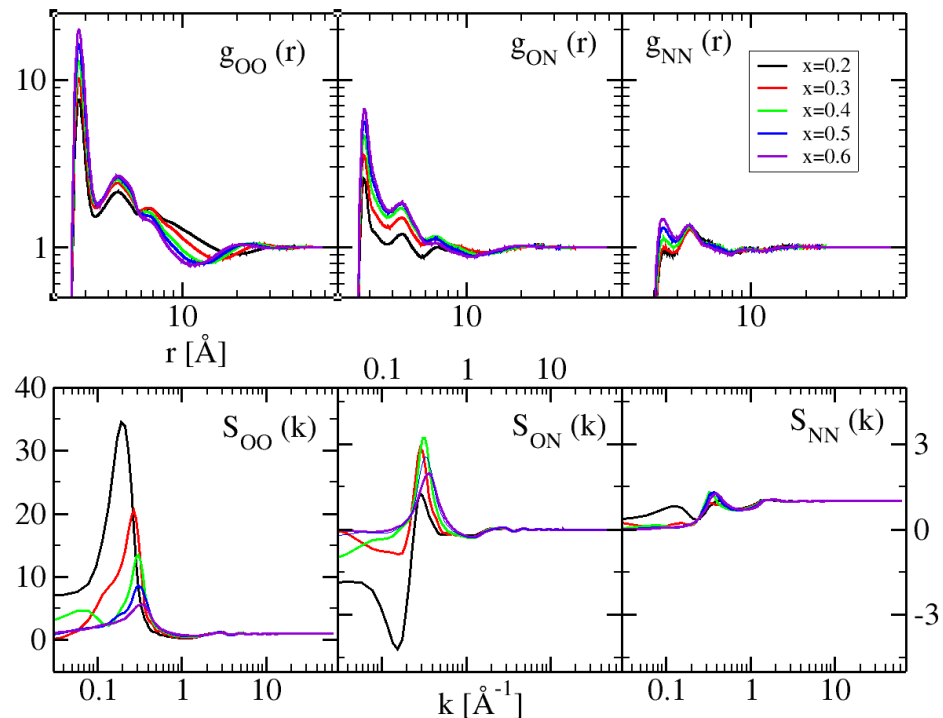


Figure 11: Hexylamine (CHARMM-AA) concentration dependence of the charged atoms O_W and N correlation functions (upper rows) and corresponding structure factors (lower rows), shown in log-log scale. The vertical scale for the middle and right lower panels is shown in the right most vertical axis, since it is different from that of the lower left panel.

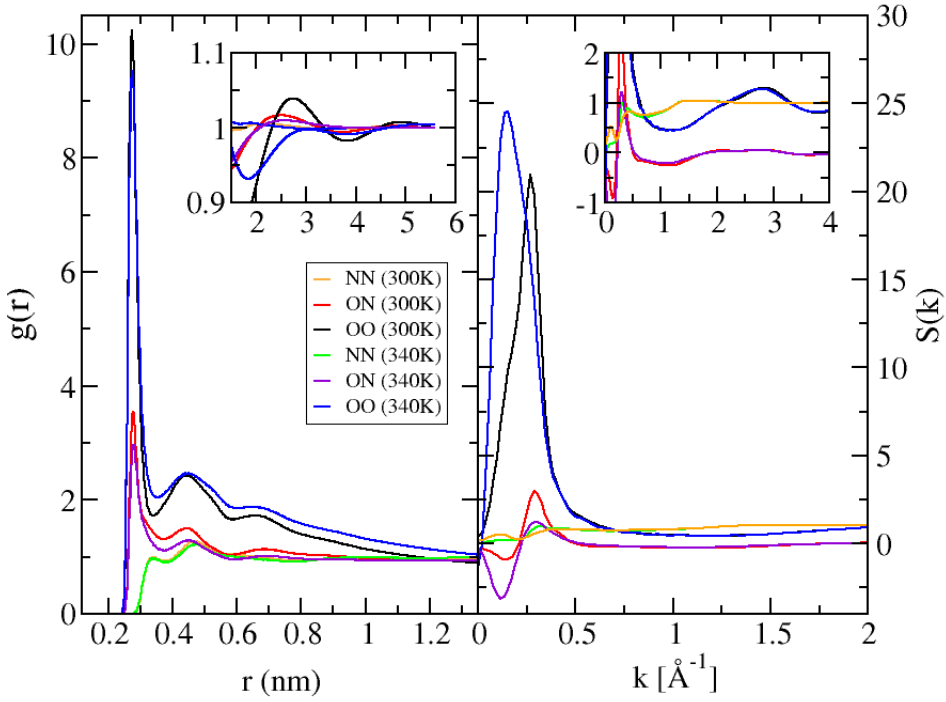


Figure 12: Temperature dependence of the pair correlation functions (left panel) and corresponding structure factors (right panel) for the 20% aqueous hexylamine mixtures. The curves for 300 K are shown in thin lines and those for the higher 340 K are shown in thicker lines. The insets show the large r (left panel) and small k (right panel) behaviour.

towards larger distances, indicating that the water domains are slightly larger at high T . The net result is a larger water pre-peak shifted towards smaller k values, witnessing the larger water domains.

The temperature dependence is generally less important than the concentration dependence. Nevertheless, our simulation results are consistent with the experimental phase diagram (see Fig.SI_1 in the SI document) which indicates that the U-shaped 2-phase region (with the LCST at the minimum of the “U”) is widening at large temperatures, supporting the observation that the water domains must be larger. This is equally supported by the x-ray experiments through the analysis of the SPP behaviour with temperature, as reported in our recent work.³ Indeed, if the water domain increase in size due to higher temperature thermal dilatation, then, at fixed amine concentration it will become harder to cover the larger surface, and demixing will occur until larger amine concentrations than at lower temperature, hence explaining the U shape curve.

6 Model dependence

So far we have examined SPC/E water with CHARMM-AA amines, except for propylamine where we have used the GROMOS force field model of our previous simulation results from.^{72,82} In our investigation we have first tried the GROMOS model, which is a UA model, and we found that it was demixing at much higher concentrations than the experimental findings. We then explored OPLS-UA which equally showed spurious demixing, then OPLS-AA which seemed better, and finally settled for CHARMM-AA, which was both qualitatively and quantitatively better. Then we tried the water TIP4P-2005 model, which is generally considered as superior to the SPC class and TIP class models. Surprisingly, we found that this water model was not so good for CHARMM-AA amines. Since our goal was not to test all possible combinations, but rather find a good compromise in order to analyze the local micro-structure, we finally settled for the SPC/E-CHARMM-AA combination.

6.1 Water model

Fig. 13 shows the charged site correlations comparing the CHARMM-AA 20% hexylamine model mixed with TIP4P-2005 water model (thick lines) and the SPC/E water model (dashed lines). It can be seen that the global trends are generally the same, with perhaps less structured water correlations in the medium distance range, as can be seen by the weaker second and third neighbour correlations of $g_{O_w O_w}(r)$ (black curves).

Also the amplitudes of the domain oscillations are somewhat smaller. These features translate into a much less well defined pre-peak for the water-water structure factor, which looks more like a $k=0$ concentration fluctuation peak. The lack of short range structure translates also in a less pronounced split main peak in the thicker black curve (right inset).

6.2 Solute models

Together with SPC/E water, we have studied four alkylamine models, namely two united atom models (where the alkyl tail methyl groups are represented as a single atom), namely OPLS-UA, GROMOS-UA, and two all atom model, namely OPLS-AA and CHARMM-AA. In a previous study⁸² we have studied the GROMOS model for aqueous propylamine and found it rather good enough to reproduce x-ray and neutron scattering data trends properly, and superior to the OPLS-UA model. However, when extending the GROMOS model to longer alkyl tails, we found that it would show clear demixing for aqueous hexylamine and octylamine at ambient conditions and 20% amine content, which is variance with the experimental data.⁷¹ Even though mixing was recovered at higher amine contents, we discarded these two models, and switched to AA models. Despite both AA models showing a good mixing trends, it was found that CHARMM-AA was in closer agreement with experimental X-ray scattering

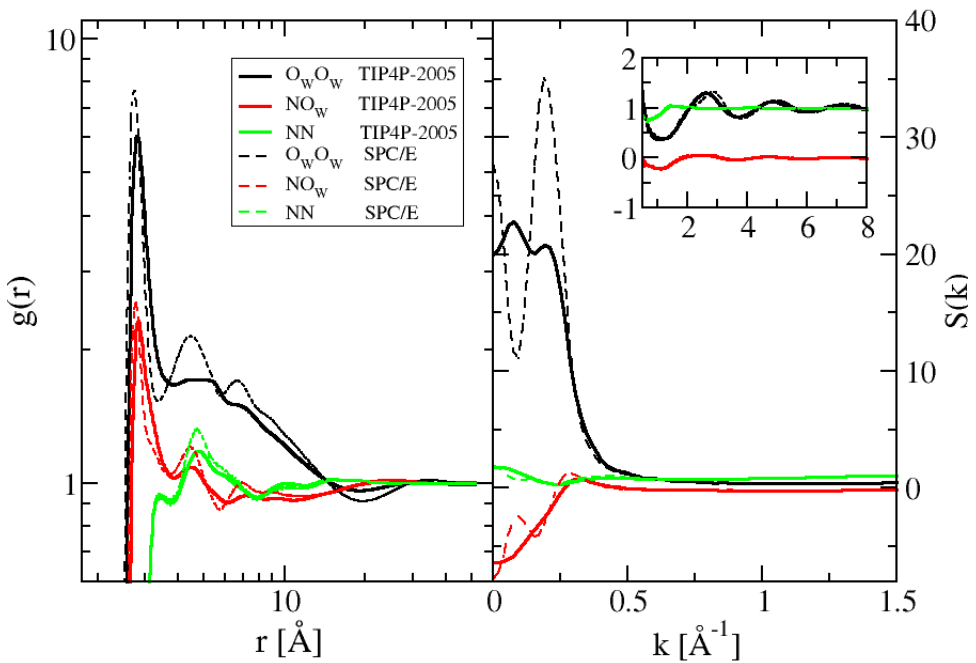


Figure 13: Water model dependence of the water oxygen atom O_W and nitrogen atom N for the case of the 20% aqueous hexylamine. The data for the TIP4P-2005 is shown in thick lines and that for the SPC/E model in dashed lines. The color conventions are in the inset of the left panel, which shows $g(r)$ function. The right panel shows the $S(k)$ functions with focus on small- k part in the main panel and large k part in the inset.

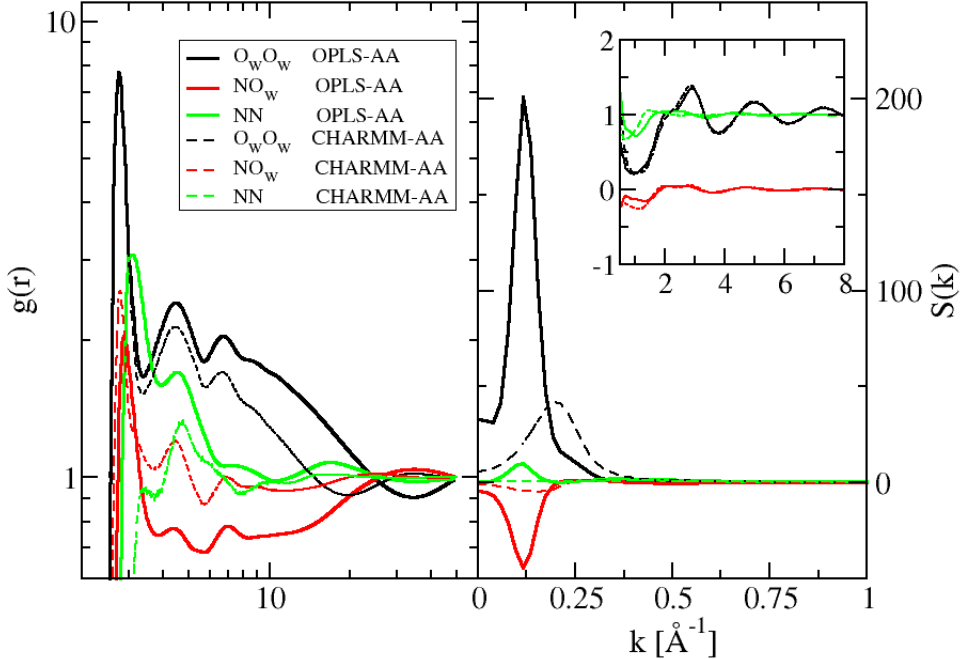


Figure 14: Alkylamine model dependence of the water oxygen atom O_w and nitrogen atom N for the case of the 20% aqueous hexylamine. The data for the OPLS-AA model of the amine is shown in thick lines and that for the CHARMM-AA model in dashed lines. The color conventions are in the inset of the left panel, which shows $g(r)$ function. The right panel shows the $S(k)$ functions with focus on small- k part in the main panel and large k part in the inset.

data, the OPLS-AA tending to overestimate the scattering pre-peak by showing stronger water-amine head group dimerising than the CHARMM-AA model.

Fig. 14 shows the 20% hexylamine aqueous mixtures correlations, comparing the OPLS-AA (thick lines) with the CHARMM-AA (dashed lines) and with SPC/E water as common solvent. OPLS-AA tends to have much better defined nitrogen atom coverage of the water domain surface. This is surprising because the partial charge on the nitrogen atom of the OPLS-AA model $q_N = -0.9$ is smaller than $q_N = -0.968$ for the CHARMM-AA model. However, the OPLS-AA model has no charges on the H and C atoms of the alkyl tail, except for the first ones.

We suggest that the strong $O_w - N$ binding in the OPLS-AA model is enforced through the neutrality of the alkyl tails. Whether this is a genuine physical effect remains debatable.

7 X-ray scattering

The experimental x-ray scattering pre-peaks are in fact the result of all the contributions from atom-atom structure factors, with some cancellations between the positive pre-peaks and negative anti-peaks. At present, it is not possible to predict the SPP for a given system without examining all atom pair contributions. When considering the scattering intensity $I(k)$, it is convenient to divide it between neighbouring atom contributions and medium/long range cluster or domain contributions. The first ones contribute mostly to the main peak of $I(k)$, whose position k_{MP} is generally related to the mean atom size, usually in the range $k_{MP} \approx 1.5 - 2 \text{\AA}^{-1}$, corresponding to the average atom van der Waals radii $\sigma \approx 2\pi/k_{MP} \approx 3 - 4 \text{\AA}$. The pre-peak is related to the mean size of the cluster/domains and is system dependent, with position $k_{PP} < k_{MP}$ between $k = 0$ and k_{MP} . The connection of k_{PP} with cluster/domain size is justified through the observation that it is related to the periodicity of the medium/large r domain oscillations. All atom-atom structure factors are affected by domain pseudo-periodicity, with however in phase oscillations between like domains, and counter-phase oscillations for cross domain correlations. The first ones contribute positively to the concerned atom-atom structure factors, while the latter contribute destructively with negative anti-peaks.

The most interesting aspect is the fact that, since the segregated domains contain the same molecular species (or those which mix well within a given domain), all corresponding atom-atom structure factors have more or less the same pre-peak features which are independent of the species atomic details, reflecting mostly domain characteristics. As a result, following Eqs.(13,14) and the Debye formula Eq.(1), one can write the radiation scattering intensity $I(k)$ as a pre-peak contribution $I_{PP}(k)$ plus a bulk one $\Delta I(k)$

$$I(k) = I_{PP}(k) + \Delta I(k) \quad (15)$$

where the SPP contribution $I_{PP}(k)$ of a binary mixture can be written solely as a species-species contributions. For the aqueous amines, one would then have, with obvious notations:

$$I_{PP}(k) = n_W^2 I_{WW}(k) + 2n_W n_A I_{WA}(k) + n_A^2 I_{AA}(k) \quad (16)$$

where $n_w = 3$ is the number of atoms for water and n_A is the number of atoms of the alkylamine molecule.

Fig. 15 illustrates these arguments for the case of 30% aqueous hexylamine. This concentration is not too close to the phase separation region, as not to be affected by concentration fluctuations, while still showing appreciable micro-segregation.

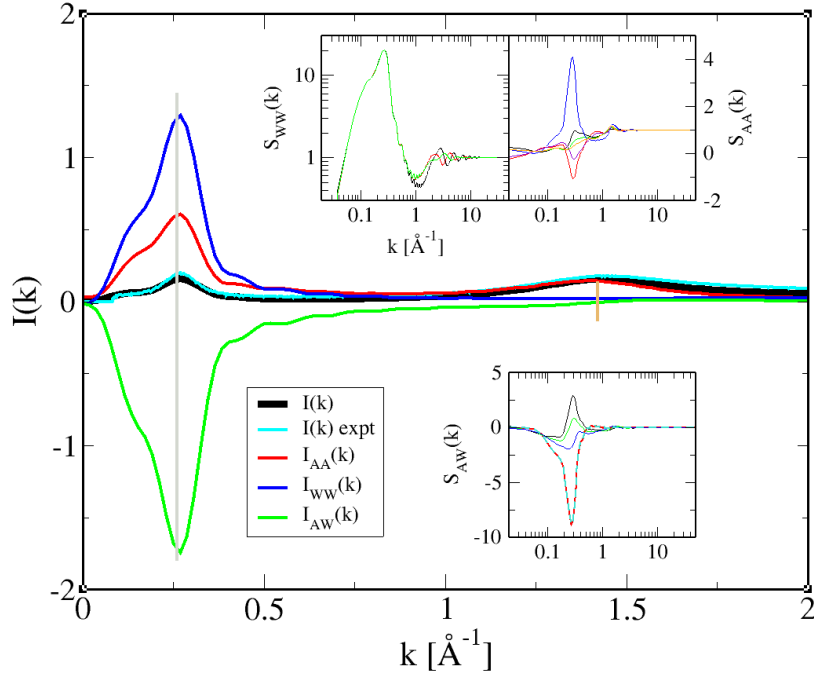


Figure 15: Scattering intensity $I(k)$ and various contributions (see text) for the case of the 30% aqueous hexylamine mixture. The experimental $I(k)$ is shown in cyan in the main panel and the calculated data in thick black. The insets show various atom-atom structure factors $S_{i,j}(k)$ (see text for details). The upper left inset is for water $S(k)$ and the upper right inset for hexylamine $S(k)$. The lower inset is for cross species $S(k)$.

The calculated (black) and the experimental (cyan) $I(k)$ are seen to be in excellent agreement for this SPC/E-CHARMM-AA model combinations. The black curve is the result of cancellations between the positive pre-peak contributions I_{WW} (blue) and I_{AA} (red) with the negative cross species anti-peak contribution I_{AW} (green). The gray vertical line indicates the position of the pre-peaks $k_{PP} \approx 0.24\text{\AA}^{-1}$ (corresponding to domain sizes of $d = 2\pi/k_{PP} \approx 25\text{\AA}$) and the light orange vertical line indicates the main peak position at $k_{MP} \approx 1.42\text{\AA}^{-1}$ (corresponding to mean atom size $\sigma = 2\pi/k_{MP} \approx 4.2\text{\AA}$, which is roughly that of the carbon atom in the CHARMM-AA model - since there are many such atoms, it is natural that the main peak position is dominated by this contribution). It is important to stress the difference in amplitude between the observed SPP and the three underlying very large positive and negative molecular contributions, which are the genuine contributions, although not observable.

The three insets show some of the atom-atom structure factors for the water (upper left inset), amine (upper right inset) and cross species (lower inset). For the water $S(k)$ it is clearly seen that all the three structure factor pre-peaks

are totally superposed, hence justifying the separation in Eq.14. The main peak contributions show differences due to different atom pair contributions. The situation is not so ideal for the two other insets, since both positive and negative contributions can be observed. However, it must be stressed that it was intentionally shown, to demonstrate that differences between pre-peaks exist in most cases. Nevertheless, the dominant contributions are from peaks that nearly superimpose, as for instance the two water- C_T correlations ($O_W - C_T$ and $H_W - C_T$) in the lower panel (cyan and red curves).

8 Discussion

The key finding of this study is the fact that stable micro-heterogeneity is obtained through the stabilizing of the domains interfaces. Indeed, this seems to be a necessary condition. In the present case, this stabilization is obtained through the strong binding of water-nitrogen pairs. Micro-heterogeneity implies the existence of clustered entities, and these can come in many dimensions, such as the linear chain-like aggregates of the hydroxyl head groups in alkanols, or domain surfaces such as in the present case. However, the presence and stabilization of such topological supra-molecular shapes necessitates that two antagonist correlations take place: the correlations between the associated charged groups and those between the charged and uncharged (or weakly charged) ones. The spatial positioning of the resulting segregated domains, which is a combination of alternation of domains with spatial disorder, is reminiscent of the charge order in ionic melts. We have previously discussed the analogy between charge order and domain order.^{53,73} The most important consequence of these microscopic molecular arrangements is the fact that the experimental observable, namely the scattering intensity is in fact a combination of the canceling between these antagonist correlations. Hence, while it is reasonable to attribute the presence of an SPP to the existence of supramolecular aggregates, what is really measured is the small remainder between the enormous real molecular contributions between the antagonist correlations.

The present approach is based on correlation functions analysis. It can be compared with “chemical” approaches, as spectroscopy, which can provide only information about short time dynamics and near neighbour positioning. This approach is likely to miss the domain formation when those are in the 1nm range. Another “chemical approach” based on the so called “polar/apolar” paradigm interprets charge order in terms of dipole order.^{83,84} Since dipole is one step lower than charge in the electrostatic order, this approach misses the domain order based on charge order. As stated in Section 2.2 the chemical approaches miss the microscopic role of density and concentration fluctuations which are fundamental random variables in a statistical approach. Conversely, the present approach does not provide deeper information about the water-nitrogen dynamics and kinetics, which are readily provided by chemical approaches. It is more suitable to analyze equilibrium structure of microscopic molecular configuration over all ranges. In addition it is very much appropriate to directly interpret

radiation scattering data.

It should be stressed that existence of clusters or supra-structure can only be searched by analyzing the various atom-atom structure factors, which can only be obtained through computer simulations of with model molecular force fields. At present, there are no “exact” force field models, hence an necessary incertitude is always present. Nevertheless, the very good agreement between calculated scattering intensities and measured ones supports the quality of the MD simulation model and helps to find proper force fields that describe the real systems in the best way. Hence, x-ray scattering experiments are a good test for the models, and the exceptional agreement reported in our recent work³ supports the assumption that the models describe the real life scenario, since the calculated intensities are well in line with the experiment in all three aspects, concentration dependence, chain length dependence and temperature dependence.

9 Conclusion

In this work, we have shown, through the analysis of the specific atom-atom density pair correlations, that the aqueous amine mixtures exhibit clear micro-heterogeneity due to the fact that the amine nitrogen atoms tend to saturate the surface of the water domains, hence stabilizing the nano-domain segregation. This is in stark contrast with the case of the aqueous alcohol mixtures, where the hydroxyl groups do not tend to stabilize the putative water domain. Hence, even though the first evidence of micro-segregation was observed in computer simulations of aqueous-methanol mixtures,⁷⁷ this micro-segregation is not stable for large alcohols, when the hydrophobic alkyl tails dominate the kinetics of the phase separation. This is the main difference between the aqueous amines and aqueous alcohol mixtures. The water oxygen and amine nitrogen pairing supports the LCST scenario proposed by Walker and Vause, and complements this scenario by the fundamental fact that this pairing leads to a stability of the segregated nano-domains. We conjecture that the stabilization of the water domains by local tight water-solute binding is the general scenario with all types of stable micro-segregation, which should also generalize to soft matter systems. This scenario allows the formation of local “molecular topological shapes” which are at the origin of the scattering pre-peaks. However, the concentration fluctuations associated with these formations are likely to shift the pre-peak positions to a $k = 0$ peak. This scenario has been recently reported for mixtures of alcohols and ionic liquids⁸⁵ , where the $k = 0$ raise is often the precursor signature of phase separation in this case. The verification of this conjecture through the theoretical approaches and simulations of models could help better understand the role of micro-heterogeneity in various systems of physico-chemical and bio-chemical interest.

Supporting Information

The Supporting Information document contains various figures complementary to those of the main paper, as well as tables of the force field charge parameters.

Acknowledgments

We thank DELTA for providing synchrotron radiation at beamline BL2 and technical support. The help of Jacqueline Savelkous, Eric Schneider, Nicola Thiering and Dirk Lützenkirchen-Hecht is thankfully acknowledged. This work was supported by the BMBF via DAAD (PROCOPE 2024-2025, Project-ID 57704875) within the French-German collaborations PROCOPE (50951YA), *Analysis of the molecular coherence in the self-assembly process: experiment and theory*.

References

- ¹ Stephenson, R. M. Mutual solubility of water and aliphatic amines. *Journal of Chemical and Engineering data* **1993**. *38*, 625–629.
- ² Walker, J. S.; Vause, C. A. Lattice theory of binary fluid mixtures: Phase diagrams with upper and lower critical solution points from a renormalization group calculation. *The Journal of Chemical Physics* **1983**. *79*, 2660–2676.
- ³ Friedrich, L.; Požar, M.; Perera, A.; Paulus, M.; Thiering, N.; Savelkous, J.; Schneider, E.; Lovrinćević; Lützenkirchen-Hecht, D.; Sternemann, C. Molecular micro-heterogeneity: Structure formation in amine-water mixtures. *unpublished* **2025**.
- ⁴ Narten, A.; Habenschuss, A. Hydrogen bonding in liquid methanol and ethanol determined by x-ray diffraction. *The Journal of Chemical Physics* **1984**. *80*, 3387–3391.
- ⁵ Sarkar, S.; Joarder, R. N. Molecular clusters and correlations in liquid methanol at room temperature. *The Journal of Chemical Physics* **1993**. *99*, 2032–2039.
- ⁶ Sarkar, S.; Joarder, R. N. Molecular clusters in liquid ethanol at room temperature. *The Journal of Chemical Physics* **1994**. *100*, 5118–5122.
- ⁷ Karmakar, A.; Krishna, P.; Joarder, R. On the structure function of liquid alcohols at small wave numbers and signature of hydrogen-bonded clusters in the liquid state. *Physics Letters A* **1999**. *253*, 207–210.
- ⁸ Vahvaselkä, K. S.; Serimaa, R.; Torkkeli, M. Determination of liquid structures of the primary alcohols methanol, ethanol, 1-propanol, 1-butanol and 1-octanol by x-ray scattering. *Journal of Applied Crystallography* **1995**. *28*, 189–195.

⁹ Yamaguchi, T.; Hidaka, K.; Soper, A. The structure of liquid methanol revisited: a neutron diffraction experiment at -80 C and +25 C. *Molecular Physics* **1999**. *96*, 1159.

¹⁰ Sahoo, A.; Sarkar, S.; Bhagat, V.; Joarder, R. N. The probable molecular association in liquid d-1-propanol through neutron diffraction. *The Journal of Physical Chemistry A* **2009**. *113*, 5160–5162.

¹¹ Tomšič, M.; Jamnik, A.; Fritz-Popovski, G.; Glatter, O.; Vlček, L. Structural properties of pure simple alcohols from ethanol, propanol, butanol, pentanol, to hexanol: Comparing monte carlo simulations with experimental sachs data. *The Journal of Physical Chemistry B* **2007**. *111*, 1738–1751.

¹² Sillrén, P.; Swenson, J.; Mattsson, J.; Bowron, D.; Matic, A. The temperature dependent structure of liquid 1-propanol as studied by neutron diffraction and epsr simulations. *The Journal of Chemical Physics* **2013**. *138*, 214501.

¹³ Požar, M.; Bolle, J.; Sternemann, C.; Perera, A. On the x-ray scattering pre-peak of linear mono-ols and the related microstructure from computer simulations. *J. Phys. Chem. B* **2020**. *124*, 8358–8371.

¹⁴ Bolle, J.; Bierwirth, S. P.; Požar, M.; Perera, A.; Paulus, M.; MÄŒenzner, P.; Albers, C.; Dogan, S.; Elbers, M.; Sakrowski, R.; et al. Isomeric effects in structure formation and dielectric dynamics of different octanols. *Phys. Chem. Chem. Phys.* **2021**. *23*, 24211–24221.

¹⁵ Požar, M.; Friedrich, L.; Millet, T.; Paulus, M.; Sternemann, C.; Perera, A. Microscopic structure of neat linear alkylamine liquids: An x-ray scattering and computer simulation study. *J. Phys. Chem. B* **2024**. *128*, 10925–10936.

¹⁶ Santos, C.; Annareddy, H. R.; Murthy, N.; Kashyap, H.; Castner, E.; Margulis, C. Temperature-dependent structure of methyltributylammonium bis(trifluoromethylsulfonyl)amide: X ray scattering and simulations. *The Journal of Chemical Physics* **2011**. *134*, 064501.

¹⁷ Siqueira, L.; Ribeiro, M. Charge ordering and intermediate range order in ammonium ionic liquids. *The Journal of Chemical Physics* **2011**. *135*, 204506.

¹⁸ Annareddy, H.; Kashyap, H.; De Biase, P.; Margulis, C. What is the origin of the prepeak in the x-ray scattering of imidazolium-based room-temperature ionic liquids? *The Journal of Physical Chemistry B* **2010**. *114*, 16838–16846. PMID: 21077649.

¹⁹ Salma, U.; Ballirano, P.; Usula, M.; Caminiti, R.; Plechkova, N. V.; Seddon, K. R.; Gontran, L. A new insight into the nanostructure of alkylammonium alkanoates based ionic liquids in water. *Physical Chemistry Chemical Physics* **2016**. *18*, 11497–11502.

²⁰ Salma, U.; Usula, M.; Caminiti, R.; Gontrani, L.; Plechkova, N. V.; Seddon, K. R. X-ray and molecular dynamics studies of butylammonium butanoate–water binary mixtures. *Physical Chemistry Chemical Physics* **2017**. *19*, 1975–1981.

²¹ PoÅŸar, M.; Bolle, J.; Dogan-Surmeier, S.; Schneider, E.; Paulus, M.; Sterne-mann, C.; Perera, A. On the dual behaviour of water in octanol-rich aqueous n-octanol mixtures: an x-ray scattering and computer simulation study. *Phys. Chem. Chem. Phys.* **2024**. *26*, 4099–4110.

²² Paturej, J.; Koperwas, K.; Tarnacka, M.; Jurkiewicz, K.; Maksym, P.; Grel-ska, J.; Paluch, M.; Kamiński, K. Supramolecular structures of self-assembled oligomers under confinement. *Soft Matter* **2022**. *18*, 4930–4936.

²³ Goddeeris, C.; Cuppo, F.; Reynaers, H.; Bouwman, W.; den Mooter, G. V. Light scattering measurements on microemulsions: Estimation of droplet sizes. *International Journal of Pharmaceutics* **2006**. *312*, 187 – 195.

²⁴ Prévost, S.; Gradzielski, M.; Zemb, T. Self-assembly, phase behaviour and structural behaviour as observed by scattering for classical and non-classical microemulsions. *Advances in Colloid and Interface Science* **2017**. *247*, 374 – 396.

²⁵ Nishikawa, K.; Iijima, T. Small-angle x-ray scattering study of fluctuations in ethanol and water mixtures. *The Journal of Physical Chemistry* **1993**. *97*, 10824–10828.

²⁶ Takamuku, T.; Saisho, K.; Nozawa, S.; Yamaguchi, T. X-ray diffraction studies on methanol-water, ethanol-water, and 2-propanol-water mixtures at low temperatures. *Journal of Molecular Liquids* **2005**. *119*, 133 – 146.

²⁷ Takamuku, T.; Maruyama, H.; Watanabe, K.; Yamaguchi, T. Structure of 1-propanol-water mixtures investigated by large-angle x-ray scattering technique. *Journal of Solution Chemistry* **2004**. *33*, 641–660.

²⁸ Perera, A.; Sokolić, F.; Almasy, L.; Koga, Y. Kirkwood-buff integrals of aqueous alcohol binary mixtures. *The Journal of chemical physics* **2006**. *124*.

²⁹ Požar, M.; Seguier, J.-B.; Guerche, J.; Mazighi, R.; Zoranić, L.; Mijaković, M.; Kežić-Lovrinčević, B.; Sokolić, F.; Perera, A. Simple and complex disorder in binary mixtures with benzene as a common solvent. *Physical Chemistry Chemical Physics* **2015**. *17*, 9885.

³⁰ Perera, A. From solutions to molecular emulsions. *Pure and Applied Chemistry* **2016**. *88*, 189.

³¹ Perera, A. *Fluctuation theory of solutions: applications in chemistry, chemical engineering, and biophysics*, CRC Press, chap. Concentration Fluctuations and Microheterogeneity in Aqueous Mixtures: New Developments in Analogy with Microemulsions, 163 – 191. **2013**.

³² Kežić, B.; Perera, A. Revisiting aqueous-acetone mixtures through the concept of molecular emulsions. *The Journal of Chemical Physics* **2012**. *137*, 134502.

³³ Kolaříková, A.; Perera, A. Concentration fluctuation/microheterogeneity duality illustrated with aqueous 1,4-dioxane mixtures. *J. Chem. Theory Comput.* **2024**. *20*, 3473–3483.

³⁴ Zoranić, L.; Sokolić, F.; Perera, A. Microstructure of neat alcohols: A molecular dynamics study. *The Journal of Chemical Physics* **2007**. *127*, 024502.

³⁵ Perera, A.; Sokolić, F.; Zoranić, L. Microstructure of neat alcohols. *Physical Review E* **2007**. *75*, 060502(R).

³⁶ Bakó, I.; Jedlovszky, P.; Pálinkás, G. Molecular clusters in liquid methanol: a reverse monte carlo study. *Journal of Molecular Liquids* **2000**. *87*, 243–254.

³⁷ Kosztolányi, T.; Bakó, I.; Pálinkás, G. Hydrogen bonding in liquid methanol, methylamine, and methanethiol studied by molecular-dynamics simulations. *The Journal of Chemical Physics* **2003**. *118*, 4546–4555.

³⁸ Lehtola, J.; Hakala, M.; Hämäläinen, K. Structure of liquid linear alcohols. *The Journal of Physical Chemistry B* **2010**. *114*, 6426–6436.

³⁹ Kusalik, P. G.; Bergman, D.; Laaksonen, A. The local structure in liquid methylamine and methylamine–water mixtures. *The Journal of Chemical Physics* **2000**. *113*, 8036–8046.

⁴⁰ Orozco, G. A.; Nieto-Draghi, C.; Mackie, A. D.; Lachet, V. Transferable force field for equilibrium and transport properties in linear, branched, and bifunctional amines i. primary amines. *The Journal of Physical Chemistry B* **2011**. *115*, 14617–14625.

⁴¹ Orozco, G. A.; Nieto-Draghi, C.; Mackie, A. D.; Lachet, V. Transferable force field for equilibrium and transport properties in linear and branched monofunctional and multifunctional amines. ii. secondary and tertiary amines. *The Journal of Physical Chemistry B* **2012**. *116*, 6193–6202.

⁴² Orozco, G. A.; Nieto-Draghi, C.; Mackie, A. D.; Lachet, V. Equilibrium and transport properties of primary, secondary and tertiary amines by molecular simulation. *Oil and Gas Science and Technology - Revue d'IFP Energies nouvelles* **2014**. *69*, 833–849.

⁴³ Orozco, G. A.; Lachet, V.; Mackie, A. D. Physical absorption of green house gases in amines: The influence of functionality, structure, and cross-interactions. *The Journal of Physical Chemistry B* **2016**. *120*, 13136–13143.

⁴⁴ Debye, P. Zerstreuung von $\text{r}\bar{\text{A}}$ ntgenstrahlen. *Annalen der Physik* **1915**. *351*, 809–823.

⁴⁵ Debye, P. Scattering of x-rays. In *The collected papers of Peter J. W. Debye*, Interscience Publishers. **1954**.

⁴⁶ Hansen, J.-P.; McDonald, I. *Theory of Simple Liquids*. Academic Press, Elsevier, Amsterdam, 3rd ed., **2006**.

⁴⁷ Lovrinčević, B.; Požar, M.; Jukić, I.; Perera, D.; Perera, A. Dynamical correlations in simple disorder and complex disorder liquids. *Journal of Molecular Liquids* **2024**. *393*, 123421.

⁴⁸ Chaikin, P. M.; Lubensky, T. C.; Witten, T. A. *Principles of condensed matter physics*, vol. 10. Cambridge university press Cambridge, **1995**.

⁴⁹ Kirkwood, J.; Buff, F. The statistical mechanical theory of solutions. i. *The Journal of Chemical Physics* **1951**. *19*, 774.

⁵⁰ Perera, A.; Požar, M.; Lovrinčević, B. Camel Back Shaped Kirkwood-Buff Integrals . *The Journal of Chemical Physics* **2022**. *156*, 124503.

⁵¹ Perera, A.; Mazighi, R. Simple and complex forms of disorder in ionic liquids. *Journal of Molecular Liquids* **2015**. *210*, 243–251.

⁵² Triolo, A.; Russina, O.; Bleif, H.-J.; Di Cola, E. Nanoscale segregation in room temperature ionic liquids. *The Journal of Physical Chemistry B* **2007**. *111*, 4641. PMID: 17388414.

⁵³ Perera, A. Charge ordering and scattering pre-peaks in ionic liquids and alcohols. *Physical Chemistry Chemical Physics* **2017**. *19*, 1062.

⁵⁴ Pronk, S.; Páll, S.; Schulz, R.; Larsson, P.; Bjelkmar, P.; Apostolov, R.; Shirts, M.; Smith, J.; Kasson, P.; van der Spoel, D.; et al. Gromacs 4.5: a high-throughput and highly parallel open source molecular simulation toolkit. *Bioinformatics* **2013**. *29*, 845–854.

⁵⁵ Oostenbrink, C.; Villa, A.; Mark, A. E.; Van Gunsteren, W. F. A biomolecular force field based on the free enthalpy of hydration and solvation: the gromos force-field parameter sets 53a5 and 53a6. *Journal of computational chemistry* **2004**. *25*, 1656–1676.

⁵⁶ Schmid, N.; Eichenberger, A.; Choutko, A.; Riniker, S.; Winger, M.; Mark, A.; van Gunsteren, W. Definition and testing of the gromos force-field versions 54a7 and 54b7. *European Biophysics Journal* **2011**. *40*, 843.

⁵⁷ Jorgensen, W.; Maxwell, D.; Tirado-Rives, J. Development and testing of the opls all-atom force field on conformational energetics and properties of organic liquids. *Journal of the American Chemical Society* **1996**. *118*, 11225.

⁵⁸ Jorgensen, W.; Madura, J.; Swenson, C. Optimized intermolecular potential functions for liquid hydrocarbons. *Journal of the American Chemical Society* **1984**. *106*, 6638–6646.

⁵⁹ Vanommeslaeghe, K.; Hatcher, E.; Acharya, C.; Kundu, S.; Zhong, S.; Shim, J.; Darian, E.; Guvench, O.; Lopes, P.; Vorobyov, I.; et al. Charmm general force field: A force field for drug-like molecules compatible with the charmm all-atom additive biological force fields. *Journal of Computational Chemistry* **2010**. *31*, 671–690.

⁶⁰ Vanommeslaeghe, K.; MacKerell, A. D. Automation of the charmm general force field (cgenff) i: Bond perception and atom typing. *Journal of Chemical Information and Modeling* **2012**. *52*, 3144–3154.

⁶¹ Vanommeslaeghe, K.; Raman, E. P.; MacKerell, A. D. Automation of the charmm general force field (cgenff) ii: Assignment of bonded parameters and partial atomic charges. *Journal of Chemical Information and Modeling* **2012**. *52*, 3155–3168.

⁶² Rizzo, R. C.; Jorgensen, W. L. Opls all-atom model for amines: Resolution of the amine hydration problem. *Journal of the American Chemical Society* **1999**. *121*, 4827–4836.

⁶³ Berendsen, H. J. C.; Grigera, J. R.; Straatsma, T. P. The missing term in effective pair potentials. *The Journal of Physical Chemistry* **1987**. *91*, 6269–6271.

⁶⁴ Abascal, J. L.; Vega, C. A general purpose model for the condensed phases of water: Tip4p/2005. *The Journal of chemical physics* **2005**. *123*.

⁶⁵ Martínez, J.; Martínez, L. Packing optimization for automated generation of complex system's initial configurations for molecular dynamics and docking. *Journal of Computational Chemistry* **2003**. *24*, 819.

⁶⁶ Bussi, G.; Donadio, D.; Parrinello, M. Canonical sampling through velocity rescaling. *The Journal of Chemical Physics* **2007**. *126*, 014101.

⁶⁷ Parrinello, M.; Rahman, A. Crystal structure and pair potentials: A molecular-dynamics study. *Physical Review Letters* **1980**. *45*, 1196.

⁶⁸ Parrinello, M.; Rahman, A. Polymorphic transitions in single crystals: A new molecular dynamics method. *Journal of Applied Physics* **1981**. *52*, 7182.

⁶⁹ Darden, T.; York, D.; Pedersen, L. Particle mesh ewald: An $n^* \log(n)$ method for ewald sums in large systems. *The Journal of Chemical Physics* **1993**. *98*, 10089.

⁷⁰ Hess, B.; Bekker, H.; Berendsen, H.; Fraaije, J. Lincs: A linear constraint solver for molecular simulations. *Journal of Computational Chemistry* **1997**. *18*, 1463.

⁷¹ Glinski, J.; Chavepeyer, G.; Platten, J.; De Saedeleer, C. Phase diagrams and interfacial properties of water-hexylamine, water-heptylamine, and water-octylamine systems. *Journal of colloid and interface science* **1994**. *162*, 129–134.

⁷² Požar, M.; Perera, A. On the micro-heterogeneous structure of neat and aqueous propylamine mixtures: A computer simulation study. *Journal of Molecular Liquids* **2017**. *227*, 210.

⁷³ Perera, A. Molecular emulsions: from charge order to domain order. *Phys. Chem. Chem. Phys.* **2017**. *19*, 28275–28285.

⁷⁴ Mijaković, M.; Kežić, B.; Zoranić, L.; Sokolić, F.; Asenbaum, A.; Pruner, C.; Wilhelm, E.; Perera, A. Ethanol-water mixtures: ultrasonics, brillouin scattering and molecular dynamics. *Journal of Molecular Liquids* **2011**. *164*, 66.

⁷⁵ Asenbaum, A.; Pruner, C.; Wilhelm, E.; Mijaković, M.; Zoranić, L.; Sokolić, F.; Kežić, B.; Perera, A. Structural changes in ethanol-water mixtures: Ultrasound, brillouin scattering and molecular dynamics studies. *Vibrational Spectroscopy* **2012**. *60*, 102.

⁷⁶ Lovrinčević, B.; Požar, M.; Friedrich, L.; Paulus, M.; Sternemann, C.; Perera, A. Aqueous-alkylamines: a continuation link between molecular emulsions and micro-emulsions. *unpublished* **2025**.

⁷⁷ Dixit, S.; Crain, J.; Poon, W.; Finney, J.; Soper, A. Molecular segregation observed in a concentrated alcohol-water solution. *Nature* **2002**. *416*, 829–832.

⁷⁸ Guo, J.-H.; Luo, Y.; Augustsson, A.; Kashtanov, S.; Rubensson, J.-E.; Shuh, D. K.; Ågren, H.; Nordgren, J. Molecular structure of alcohol-water mixtures. *Physical Review Letters* **2003**. *91*, 157401.

⁷⁹ Allison, S.; Fox, J.; Hargreaves, R.; Bates, S. Clustering and microimmiscibility in alcohol-water mixtures: Evidence from molecular-dynamics simulations. *Physical Review B* **2005**. *71*, 024201.

⁸⁰ Gupta, R.; Patey, G. N. Aggregation in dilute aqueous tert-butyl alcohol solutions: Insights from large-scale simulations. *The Journal of Chemical Physics* **2012**. *137*, 034509.

⁸¹ Požar, M.; Lovrinčević, B.; Zoranić, L.; Primorac, T.; Sokolić, F.; Perera, A. Micro-heterogeneity versus clustering in binary mixtures of ethanol with water or alkanes. *Physical Chemistry Chemical Physics* **2016**. *18*, 23971.

⁸² Almásy, L.; Kuklin, A.; Požar, M.; Baptista, A.; Perera, A. Microscopic origin of the scattering pre-peak in aqueous propylamine mixtures: X-ray and neutron experiments versus simulations. *Phys. Chem. Chem. Phys.* **2019**. *21*, 9317–9325.

⁸³ Russina, O.; Sferrazza, A.; Caminiti, R.; Triolo, A. Amphiphile meets amphiphile: Beyond the polar-apolar dualism in ionic liquid/alcohol mixtures. *The Journal of Physical Chemistry Letters* **2014**. *5*, 1738–1742. PMID: 26270376.

⁸⁴ Kashyap, H. K.; Hettige, J. J.; Annapureddy, H. V.; Margulis, C. J. Saks anti-peaks reveal the length-scales of dual positive–negative and polar–apolar ordering in room-temperature ionic liquids. *Chemical Communications* **2012**. *48*, 5103–5105.

⁸⁵ Jiang, H. J.; FitzGerald, P. A.; Dolan, A.; Atkin, R.; Warr, G. G. Amphilic self-assembly of alkanols in protic ionic liquids. *The Journal of Physical Chemistry B* **2014**. *118*, 9983–9990.